26. THE EFFECT OF INCREASING CO_2 ON THE EXTREME SEPTEMBER 2016 RAINFALL ACROSS SOUTHEASTERN AUSTRALIA

Pandora Hope, Eun-Pa Lim, Harry Hendon, and Guomin Wang

The effect of increasing atmospheric CO_2 on the extreme September 2016 rainfall across southeastern Australia was minimal, with changes in circulation and static stability driving a tendency towards drier conditions.

Introduction. In 2016 Australia experienced extreme, widespread rainfall, with flooding and wild weather impacting some agriculture and power generation. It was particularly wet through winter and into early spring, with the wettest September for eastern Australia ever recorded (Bureau of Meteorology 2016a,b; King 2017; Fig. 26.1d).

Extreme rainfall on a range of time scales is expected to become more extreme in a warmer world (e.g., Allan and Soden 2008; Held and Soden 2006) particularly at subdaily time scales (Westra et al. 2014), but also on daily (CSIRO and Bureau of Meteorology 2015) and monthly time scales (Watterson et al. 2016). Observed trends toward higher intensity rainfall have been found in many regions around the globe (Westra et al. 2013). While thermodynamic arguments alone might suggest that rainfall will increase in a warmer world, the circulation will also respond due to a range of factors (Bony et al. 2013; Colman and McAvaney 1997; He and Soden 2016; Johnson and Xie 2010; Seager et al. 2010; Vecchi et al. 2006), generally working to reduce rainfall in the subtropics.

In Australia, while there is some indication that the intensity of subhourly rainfall is increasing (Chen et al. 2013; Westra and Sisson 2011), the signal is not clear on daily or longer time scales (Gallant et al. 2012).

However, attribution studies of extreme events can elucidate the role of increasing levels of atmospheric CO_2 on extreme rainfall. The extreme rainfall across eastern Australia in September 2016 provides an excellent case study to help understand how increasing CO_2 is influencing extreme rainfall in Australia.

The event. Across central and eastern Australia, many regions had their highest September rainfall on record in 2016, resulting in the wettest September for eastern Australia ever recorded with an average of 84.0 mm, 8.9 mm greater than the previous record and more than three times the mean. It was the wettest September on record for New South Wales and the Northern Territory, as well as for the Murray–Darling basin (MDB) in southeastern Australia, Australia's "food-bowl" (Fig. 26.1d).

In this study, we focus on the important agricultural MDB region, which covers most of the noncoastal southeast, and a particular two-week period, [15–28 September] when various climate features were skillfully predicted by the Australian Bureau of Meteorology's dynamical forecast system, POAMA2, which is the base model for this investigation. For the MDB, these two weeks in 2016 were the second wettest on record (compared to all 15–28 September periods) with a sum of 49.3 mm of rain, for comparison with model results, the anomaly was +2.8 mm day^{-1}, compared to the 2000–14 average of 0.7 mm day^{-1}. Thus these two weeks in September 2016 provide an excellent example of an extreme rainfall episode to examine the influence from increasing levels of CO_2.

At the time in 2016, all of the key climate drivers of eastern Australian rainfall were in a state that would favor wet conditions (e.g., Lim et al. 2016). The Indian Ocean Dipole (IOD) of September 2016 was strongly negative (Lim and Hendon 2017), with its eastern node the second warmest on record (ERSSTv4 data; www.bom.gov.au/climate/enso/wrap-up/archive/20161011.archive.shtml). Also, the September 2016 Southern Oscillation Index (SOI) was strongly positive (13.5; www.bom.gov.au/climate/current/soihtm1.shtml)

AFFILIATIONS: Hope, Lim, Hendon, and Wang—Bureau of Meteorology, Melbourne, Victoria, Australia

DOI:10.1175/BAMS-D-17-0094.1

A supplement to this article is available online (10.1175/BAMS-D-17-0094.2)

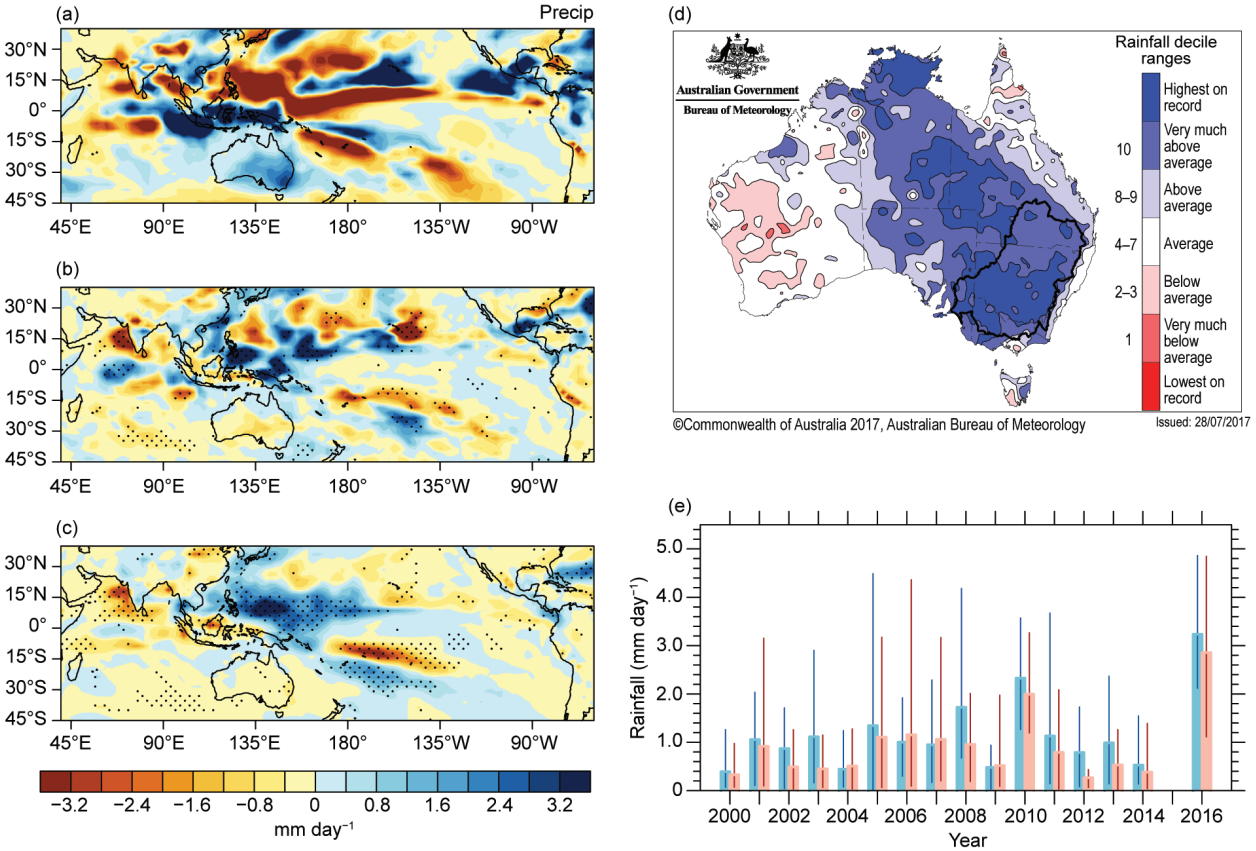

Fig. 26.1. (a) Forecast rainfall anomaly (mm day^{-1}) from 2000–14 climatology) for 15–28 Sep 2016, using 11 members of model version a. (b) Difference between 2016 forecast rainfall (mm day^{-1}) under current levels of CO_2 (401.03 ppm; www.esrl.noaa.gov/gmd/ccgg/trends/data.html) and 1960 CO_2 levels (315 ppm), using 11 members of model versions a,b,c (33 total). (c) Climatological rainfall difference (mm day^{-1}) for current minus low CO_2 levels, using 11 members of model version a. Stippling in (b) and (c) indicates significant differences (10% level). (d) Outline of MDB region, over rainfall deciles for Sep 2016 (relative to 1901–2016), and (e) ensemble mean rainfall forecast (mm day^{-1}) time series for last two weeks of Sep under current (red bars) and low CO_2 (blue bars) conditions for MDB region. Lines show ensemble spread across 11 members.

and Niño-3.4 was at near-La Niña levels, depending on the definition (Lim and Hendon 2017). SAM was strongly positive in the first three weeks of September 2016 but weakened later in the month (www.cpc.ncep.noaa.gov/products/precip/CWlink/daily_ao_index/aao/aao.shtml). The intensity of the IOD negative was found to be important for the high rainfall across Australia in 2016 (King 2017). In this study, we particularly focus on the factors that contribute to local rainfall generation including high humidity, unstable conditions, and favorable circulation.

Method. POAMA2 is the operational seasonal forecast system of the Australian Bureau of Meteorology (Wang et al. 2005). It has the BAM3 atmospheric model, (T47, L17; Colman et al. 2005), ACOM2 ocean model (Schiller et al. 2002) with a resolution of 2° longitude and a telescoping meridional resolution of 0.5° equatorward of 8° latitude, gradually increasing to 1.5° near the poles and 25 levels.

POAMA2 forecasts are initialized with realistic atmosphere, land, and ocean conditions that are generated from separate atmosphere/land surface (Hudson et al. 2011) and ocean (Yin et al. 2011) data assimilation systems. Sea–ice and ozone are set to their respective climatological annual cycles. Ensembles of 11 are produced using perturbed initial conditions with a coupled breeding technique (Hudson et al. 2013). Three versions of the model (called a, b, c) are used to increase the ensemble to 33 members. Model versions a and c differ in their boundary layer physics, and b is the flux-corrected version (Cottrill et al. 2013).

Thirty-three-member ensemble forecasts were initialized on 8 September with realistic atmosphere (including observed CO_2 concentration), ocean, and

land conditions, and verified for 15–28 September 2016. POAMA2 generally captures September rainfall in the MDB well (Langford and Hendon 2013), and these two particular weeks were chosen because not only was the rainfall forecast well (Fig. 26.1a), but the important, strong negative IOD and associated circulation were also forecast very well (Figs. ES26.1a,d). A second, "low CO_2", 33-member ensemble forecast was initialized with the same initial conditions, but with the influence of the last 55 years of CO_2 increase removed following Hope et al. (2016) and Wang et al. (2016). The CO_2 signal removed from the initial conditions was calculated for the ocean first (D_{ocean}), being the difference of the last five years of two sets of 30-year, free-running simulations with atmospheric CO_2 set to 1960 (315 ppm) or 2014 (~400 ppm) values. The anomalies D_{atmos} and D_{land} were calculated from the restart files valid at the end of two-month forecasts initialized with either observed initial conditions or those with D_{ocean} removed, and corresponding levels of atmospheric CO_2.

Two sets of hindcasts were generated for the period 2000–14 to compute the two climatologies that represent the climate states with current and low CO_2 using the same experimental method as described above, but only using version a of POAMA2 (Fig. 26.1e), resulting in 165 forecasts. The climatological pattern of change in SSTs (Fig. ES26.1c) aligns with the observed warming seen across the globe in the CMIP5 climate models, with particular alignment to those forced with only greenhouse gases (Bindoff et al. 2013).

To determine how increasing levels of CO_2 alter rainfall through circulation changes, we analyze the components of the moisture budget as done in Seager et al. (2010). They propose that the changes in the moisture budget due to increasing CO_2 are caused thermodynamically by changes in specific humidity and dynamically by changes in circulation. The thermodynamic and dynamic contributions are further separated into advective and divergent components. In our analysis for the last two weeks of September 2016, we found that the change in the moisture budget due to the change of wind divergence largely explained the forecast pattern of rainfall change produced under differing levels of CO_2. Therefore, we focus on the moisture transport by the CO_2-induced change of wind divergence.

Did increased atmospheric CO_2 alter the rainfall amount? The ensemble mean forecast 2016 rainfall anomaly under current levels of CO_2 (Fig. 26.1a) shows wet conditions across all of Australia. The area mean forecast anomaly for the model MDB region (25°–40°S, 140°–156°E) is +2.1 mm day^{-1}, similar to the observed anomaly of +2.7 mm day^{-1}, and the wettest in the modeled climatology (red bar at 2016 in Fig. 26.1e). Other forecast features align with observed conditions, including the heavy rain and the high sea surface temperatures (Fig. ES26.1a) to the north of Australia associated with the negative IOD, weak La Niña, and the pressure anomalies associated with positive SAM (http://poama.bom.gov.au/).

The rainfall forecast under low levels of CO_2 is slightly higher than under current levels of CO_2, thus the forecast rain under current conditions minus that under 1960 CO_2 levels (Fig. 26.1b) is slightly drier over most of the continent. The difference over the MDB region is −0.35 mm day^{-1}. The impact of CO_2 on the 2016 forecasts resembles the underlying rainfall change due to the last 55 years of CO_2 increase as shown by the September 2000–14 climatological difference in current minus low CO_2 rainfall (Figs. 26.1c,e), confirming that our 2016 experiments capture the modeled canonical response to changing CO_2 levels. This analysis suggests that the rainfall might have been even greater without increased levels of CO_2, although the difference is not statistically significant (at 10% level).

We next briefly explore whether there was a shift in the intensity of the daily rainfall. The frequency distributions of predicted daily rainfall intensities for both 2016 (Fig. ES26.2a) and the climatology (Fig. ES26.2b) do differ between forecasts under current or low CO_2 conditions. We see a greater proportion of days with very little rainfall (0–1.5 mm day^{-1}) and reduced proportion of days with moderate rainfall (2–5 mm day^{-1}) under current CO_2 levels. There are no discernible differences in the tails of the distributions of either the predicted event or the climatologies (Fig. ES26.2). The structure of this shift might mean that under current conditions, greater energy is required to instigate rainfall, but this could be pursued in a further study.

Did increased CO_2 alter the physical processes responsible for the rainfall? To better understand the regional physical processes responsible for the high rainfall in 2016 and their response to CO_2, we consider the forecast changes in available moisture, the circulation, and the atmospheric stability. The forecast 2016 precipitable water was extremely high over north and eastern Australia (Fig. 26.2a), moisture convergence over eastern Australia was strong (Fig. 26.2b: note

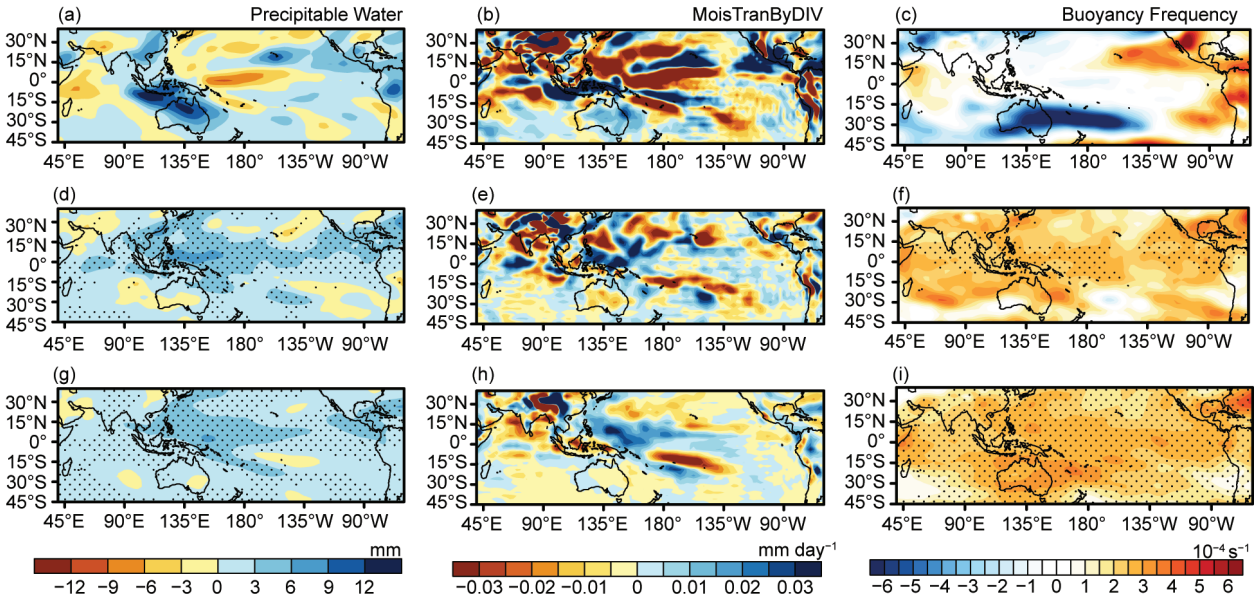

Fig. 26.2. (a) Precipitable water anomaly (mm), (b) moisture transport by divergence of anomalous winds (mm day^{-1}), and (c) midlevel (700–300 hPa) atmospheric stability as shown by buoyancy term, N (s^{-1}) of 15–28 Sep 2016 forecast anomaly (from 2000–14 climatology) (top panels). (d)–(f) Same as (a)–(c) but of difference in 2016 forecast with current and 1960 CO_2 conditions (middle panels). (g)–(h) The same as (a)–(c) but of climatological difference for current minus 1960 CO_2 levels. Stippling in left and right panels indicates statistically significant differences (10% level).

units of mm day^{-1}), and static stability was decreased as evidenced by large negative anomalies of midlevel atmospheric buoyancy (N) extending across Australia (Fig. 26.2c).

For these weeks in September, the influence resulting from the last 55 years of increasing CO_2 acted to increase the forecast precipitable water through most of the tropics including northern Australia (Fig. 26.2d), but there was little change over the MDB region. This is consistent with the current minus low CO_2 climatological difference (2000–14) in precipitable water (Fig. 26.2g). From the moisture budget analysis of the 2016 forecasts, the CO_2-induced change of moisture transport by wind divergence led to drying over southeast Australia, more so than in the climatological difference (Fig. 26.2h). Higher static stability was also simulated across Australia with increasing levels of CO_2 in 2016 (Fig. 26.2f), though this shift was weaker than that in the climatological difference (Fig. 26.2i). CMIP5 ALL-forcing historical simulations for 1960–2010 show atmospheric responses indicative of increased static stability, with a stronger warming trend in the upper troposphere (~0.35°C decade^{-1}) than in the lower troposphere (~0.27°C decade^{-1}) in the region of 20°S–20°N (Bindoff et al. 2013), which is weaker but still consistent with the temperature response in POAMA2 experiments shown here, possibly as these are forced with the CO_2 change only.

Concluding remarks. A drier future is projected for the MDB in September at the end of the century by most climate models (CSIRO and Bureau of Meteorology, 2015; Hope et al. 2015), and results suggest that increasing levels of CO_2 over the last 55 years have already led to circulation and stability changes that would promote slightly drier conditions than in the 1960s, even for an extreme, two-week rainfall event. This study highlights the influence of changing levels of CO_2 alone, perhaps thus aligning more strongly with expected future changes and historical trends in models forced only with greenhouse gases compared to those attribution methods or models with all forcings (Bindoff et al. 2013).

ACKNOWLEDGMENTS. We thank our editor Carl Schreck, Marty Hoerling, two anonymous reviewers, and two internal reviewers, Hanh Nguyen and Christine Chung, for their suggestions that led to an improved manuscript. This project was in part supported through funding from the Australian Government's National Environmental Science Programme.

REFERENCES

Allan, R. P., and B. J. Soden, 2008: Atmospheric warming and the amplification of precipitation extremes. *Science*, **321**, 1481–1484, doi:10.1126/science.1160787 .

Bindoff, N. L., and Coauthors, 2013: Detection and attribution of climate change: From global to regional. *Climate Change 2013: The Physical Science Basis*, T. F. Stocker et al., Eds., Cambridge University Press, 867–952.

Bony, S., G. Bellon, D. Klocke, S. Sherwood, S. Fermepin, and S. Denvil, 2013: Robust direct effect of carbon dioxide on tropical circulation and regional precipitation. *Nat. Geosci*., **6**, 447–451, doi:10.1038/ngeo1799.

Bureau of Meteorology, 2016a: Special Climate Statement 57: Extensive early June rainfall affecting the Australian east coast. Bureau of Meteorology, 20 pp. [Available online at www.bom.gov.au/climate/current/statements/scs57.pdf.]

——, 2016b: Special Climate Statement 58: Record September rains continue wet period in much of Australia. Bureau of Meteorology, 31 pp. [Available online at www.bom.gov.au/climate/current/statements/scs58.pdf.]

Chen, Y.-R., B. Yu, and G. Jenkins, 2013: Secular variation in rainfall intensity and temperature in estern Australia. *J. Hydrometeor*., **14**, 1356–1363, doi:10.1175/JHM-D-12-0110.1.

Colman, R. A., and B. J. McAvaney, 1997: A study of general circulation model climate feedbacks determined from perturbed sea surface temperature experiments. *J. Geophys. Res*., **102**, 19383–19402, doi:10.1029/97JD00206.

——, and Coauthors, 2005: BMRC atmospheric model (BAM) version 3.0: Comparison with mean climatology. BMRC Research Rep. 108, Bureau of Meteorology Research Centre, 32 pp.

Cottrill, A., and Coauthors, 2013: Seasonal forecasting in the Pacific using the coupled model POAMA-2. *Wea. Forecasting*, **28**, 668–680, doi:10.1175/WAF-D-12-00072.1.

CSIRO and Bureau of Meteorology, 2015: *Climate Change in Australia: Projections for Australia's NRM Regions*. CSIRO and Bureau of Meteorology, Australia, 216 pp. [Available online at www.climatechangeinaustralia.gov.au/en/publications-library/technical-report/.]

Gallant, A. J. E., A. S. Kiem, D. C. Verdon-Kidd, R. C. Stone, and D. J. Karoly, 2012: Understanding climate processes in the Murray-Darling basin for natural resources management. *Hydrol. Earth Syst. Sci*., **16**, 2049–2068, doi:10.5194/hess-16-2049-2012.

He, J., and B. J. Soden, 2016: A re-examination of the projected subtropical precipitation decline. *Nat. Climate Change*, **7**, 53–57, doi:10.1038/nclimate3157.

Held, I. M., and B. J. Soden, 2006: Robust responses of the hydrological cycle to global warming. *J. Climate*, **19**, 5686–5699, doi:10.1175/JCLI3990.1.

Hope, P., and Coauthors, 2015: Seasonal and regional signature of the projected southern Australian rainfall reduction. *Aust. Meteor. Oceanogr. J*., **65**, 54–71. [Available online at www.bom.gov.au/jshess/docs/2015/hope1.pdf.]

——, G. Wang, E.-P. Lim, E.-P., H. H. Hendon, and J. M. Arblaster, 2016: What caused the record-breaking heat across Australia in October 2015? [in "Explaining Extreme Events of 2015 from a Climate Perspective"]. *Bull. Amer. Meteor. Soc*., **97** (12), S122–S126, doi:10.1175/BAMS-D-16-0142.1.

Hudson, D., O. Alves, H. H. Hendon, and G. Wang, 2011: The impact of atmospheric initialisation on seasonal prediction of tropical Pacific SST. *Climate Dyn*., **36**, 1155–1171, doi:10.1007/s00382-010-0763-9.

——, A. G. Marshall, Y. Yin, O. Alves, and H. H. Hendon, 2013: Improving intraseasonal prediction with a new ensemble generation strategy. *Mon. Wea. Rev*., **141**, 4429–4449, doi:10.1175/MWR-D-13-00059.1.

Johnson, N. C., and S.-P. Xie, 2010: Changes in the sea surface temperature threshold for tropical convection. *Nat. Geosci*., **3**, 842–845, doi:10.1038/ngeo1008.

King, A., 2017: Natural variability not climate change drove the record wet winter in southeast Australia. *Bull. Amer. Meteor. Soc*., **99** (1), S139–S143, doi:10.1175/BAMS-D-0087.1.

Langford, S., and H. H. Hendon, 2013: Improving reliability of coupled model forecasts of Australian seasonal rainfall. *Mon. Wea. Rev*., **141**, 728–741, doi:10.1175/MWR-D-11-00333.1.

Lim, E.-P., and H. H. Hendon, 2017: Causes and predictability of the negative Indian Ocean dipole and its impact on La Niña during 2016. *Sci. Rep*., **7**, 12619, doi:10.1038/s41598-017-12674-z.

——, ——, J. M. Arblaster, C. Chung, A. F. Moise, P. Hope, G. Young, and M. Zhao, 2016: Interaction of the recent 50 year SST trend and La Nina 2010: Amplification of the Southern Annular Mode and Australian springtime rainfall. *Climate Dyn*., **47**, 2273–2291, doi:10.1007/s00382-015-2963-9.

Schiller, A., J. S. Godfrey, P. C. McIntosh, G. A. Meyers, N. R. Smith, O. Alves, G. Wang, and R. Fiedler, 2002: A new version of the australian community ocean model for seasonal climate prediction. CSIRO Marine Research Rep. 240, 82 pp., doi:10.4225/08/585c1671163bd.

Seager, R., N. Naik, N., and G. A. Vecchi, 2010: Thermodynamic and dynamic mechanisms for large-scale changes in the hydrological cycle in response to global warming. *J. Climate*, **23**, 4651–4668, doi:10.1175/2010JCLI3655.1.

Vecchi, G. A., B. J. Soden, A. T. Wittenberg, I. M. Held, A. Leetmaa, and M. J. Harrison, 2006: Weakening of tropical Pacific atmospheric circulation due to anthropogenic forcing. *Nature*, **441**, 73–76, doi:10.1038/nature04744.

Wang, G., O. Alves, and N. Smith, 2005: BAM3.0 tropical surface flux simulation and its impact on SST drift in a coupled model. BMRC Research Rep. 107, 30 pp.

——, P. Hope, E.-P. Lim, H. H. Hendon, and J. M. Arblaster, 2016: Three methods for the attribution of extreme weather and climate events. Bureau of Meteorology Res. Rep. 018, 31 pp. [Available online at www.bom.gov.au/research/publications/researchreports/BRR-018.pdf.]

Watterson, I. G., Z.-W. Chua, and P. K. Hope, 2016: Extreme monthly rainfall over Australia in a changing climate. *J. South. Hemisphere Earth Syst. Sci.*, **66**, 402–423, doi:10.22499/3.6604.003.

Westra, S., and S. A. Sisson, 2011: Detection of non-stationarity in precipitation extremes using a max-stable process model. *J. Hydrol.*, **406**, 119–128, doi:10.1016/j.jhydrol.2011.06.014.

——, L. V. Alexander, and F. W. Zwiers, 2013: Global increasing trends in annual maximum daily precipitation. *J. Climate*, **26**, 3904–3918, doi:10.1175/JCLI-D-12-00502.1.

——, and Coauthors, 2014: Future changes to the intensity and frequency of short-duration extreme rainfall. *Rev. Geophys.*, **52**, 522–555, doi:10.1002/2014RG000464.

Yin, Y., O. Alves, and P. R. Oke, 2011: An ensemble ocean data assimilation system for seasonal prediction. *Mon. Wea. Rev.*, **139**, 786–808, doi:10.1175/2010MWR3419.1.